

The Low X-Ray State of LS 5039 / RX J1826.2-1450

A. Martocchia¹, C. Motch¹, I. Negueruela²

¹ CNRS / Observatoire Astronomique de Strasbourg, 11 rue de l'Université, F-67000 Strasbourg, France

² Departamento de Física, Ingeniería de Sistemas y Teoría de la Señal, Escuela Politécnica Superior, University of Alicante, Ap. 99, E-03080 Alicante, Spain

Received... Accepted...

Abstract. Recent *XMM-Newton* and *Chandra* observations of the high mass X-ray binary LS 5039 / RX J1826.2-1450 caught the source in a faint X-ray state. In contrast with previous *RXTE* observations, we fail to detect any evidence of iron line emission. We also fail to detect X-ray pulsations. The X-ray spectrum can be well fitted by a simple powerlaw, slightly harder than in previous observations, and does not require the presence of any additional disk or blackbody component. *XMM-Newton* data imply an X-ray photoelectric absorption ($N_{\text{H}} \sim 7 \times 10^{21} \text{ cm}^{-2}$) consistent with optical reddening, indicating that no strong local absorption occurs at the time of these observations. We discuss possible source emission mechanisms and hypotheses on the nature of the compact object, giving particular emphasis to the young pulsar scenario.

Key words. Stars: individuals: LS 5039, RX J1826.2-1450 – X-rays: binaries

1. Introduction

LS 5039/RX J1826.2-1450 is a massive X-ray binary (HMXB) identified in the *ROSAT* all-sky survey by Motch et al. (1997). The dynamical parameters of this source, as well as the hardness of its X-ray emission, are consistent with the compact object being either a neutron star (NS) or a black hole (BH). It may be accreting directly from the companion's wind, but the presence of an accretion disk has not been excluded yet.

Optical observations (Motch et al. 1997) allowed the identification of the optical counterpart, a bright $V = 11.2$, $O6.5V((f))$ star (Clark et al. 2001). The optical photometric variability is very small (< 0.01 mag, Martí et al. 2004) and optical colours yield $E(B - V) \sim 1.26$ (Motch et al. 1997), which implies (according to the empirical formulae in Predehl & Schmitt 1995) $N_{\text{H}} \sim 7.2 \times 10^{21} \text{ cm}^{-2}$. The source distance has been estimated at about 3.1 kpc (Motch et al. 1997), a value confirmed by Ribó et al. (2002) and adopted throughout this work.

The binary parameters were inferred spectroscopically for the first time by McSwain et al. (2001): they found a period $P_{\text{orb}} = 4.117 \pm 0.011$ d (now revised: 4.4267 ± 0.0005 d) and a high eccentricity ($e = 0.48 \pm 0.06$; McSwain et al., 2004). The mass function is quite low ($f(m) = 0.0017 \pm 0.0005 M_{\odot}$), yielding a lowest acceptable inclination $i > 9^{\circ}$ and a compact object mass $M_{\text{co}} < 8 M_{\odot}$. $O6.5V((f))$ stars

typically have $M \sim 36 M_{\odot}$ and $R \sim 10 R_{\odot}$ (Howarth & Prinja 1989).

Interestingly, LS 5039 is a runaway system, escaping from the Galactic plane with a total systemic velocity of $\sim 150 \text{ km s}^{-1}$ and a perpendicular component greater than 100 km s^{-1} with respect to the plane itself (Ribó et al. 2002; McSwain & Gies 2002).

First hints of radio emission from LS 5039 were given by the VLA (Martí et al. 1998); afterwards, a GBI-NASA monitoring campaign (Ribó et al. 1999) showed a moderate radio variability, with a clear non-thermal spectral index and no bursting activity. More recently, VLBA observations at milliarcsecond scales revealed persistent emission from radio jets (Paredes et al. 2000, 2002): therefore, the source is usually referred to as one of the few known *microquasars*, and is one of the very few radio-emitting massive X-ray binaries. The VLBA map shows bipolar jets, emerging for at least 6 milli-arcseconds from a central core.

The source may have been detected in the γ -ray band ($E > 100 \text{ MeV}$): an association with the *EGRET* source 3EG J1824-1514 has been proposed (Paredes et al. 2000, 2002) and discussed in the framework of a model in which photons are up-scattered by the relativistic electrons in a cylindrical inhomogeneous jet (Bosch-Ramon & Paredes 2004)

A broad emission line was seen in *Rossi-XTE* PCA data at $E_0 \sim 6.6 \text{ keV}$ (Ribó et al. 1999), compatible with

a slightly blue-shifted, fluorescent neutral iron feature, or with Fe XXV emission at rest velocity. This detection is of utmost interest, since fluorescent iron line emission can be used as a powerful diagnostic to test assumptions on the accretion flow and/or the jet; however, the PCA energy resolution is insufficient to distinguish between the possible models for the line. Also for this reason, observations of LS 5039 / RX J1826.2-1450 with the new generation X-ray satellites are of great importance.

In the present work we therefore concentrate on recently obtained *Chandra* and *XMM-Newton* data. After summarising the results obtained with previous X-ray missions (next Section), we describe the new data (Section 3), and discuss the implications in the last Section.

Observation	$F_{0.3-10\text{keV}}$	Orbital Phase	Γ
<i>RXTE</i> 08/02/98 (I)	~ 40	~ 0.91	1.95 ± 0.02
<i>RXTE</i> 08/02/98 (II)	~ 40	~ 0.10	1.95 ± 0.02
<i>RXTE</i> 16/02/98	~ 40	~ 0.88	1.95 ± 0.02
<i>ASCA</i> 04/10/99	~ 13	0.22-0.38	~ 1.5
<i>SAX</i> 08/10/00	~ 4.9	0.75-0.96	$\lesssim 1.8$
<i>Chandra</i> 10/09/02	~ 8.1	~ 0.35	$1.15^{+0.23}_{-0.21}$
<i>XMM</i> 08/03/03	~ 10.3	~ 0.79	$1.56^{+0.02}_{-0.05}$
<i>XMM</i> 27/03/03	~ 9.7	~ 0.21	$1.49^{+0.05}_{-0.04}$

Table 1. X-ray unabsorbed flux in the 0.3–10 keV band (in units of 10^{-12} erg cm $^{-2}$ s $^{-1}$), orbital phase and spectral powerlaw index of LS 5059 in the observations performed with different satellites. The references for the *RXTE* and *BeppoSAX* observations are Ribó et al. (1999) and Reig et al. (2003), respectively; however, we checked PDS data ourselves to better constrain Γ in the *BeppoSAX* observation (see text). We also analyzed *ASCA* SIS and GIS data, obtaining the results which are reported here. Orbital phases are computed according to the revised ephemeris of McSwain et al. (2004); the associated errors range from 2 to 5%.

2. The X-Ray History of RX J1826.2-1450

A first detection of LS 5039’s X-ray emission was given by *ROSAT* (Motch et al. 1997), which found the source at a luminosity level $L_X \sim 8.1 \times 10^{33}$ erg s $^{-1}$ in the 0.1–2.4 keV interval.

Rossi-XTE ASM data, covering the period 1996 February – 1998 November, and PCA data obtained in 1998 were analysed by Ribó et al. (1999). They found no evidence of any X-ray periodicities (on timescales 2–200 d and 0.02–2000 s, respectively), nor of any significant variation on the two-year timescale. PCA data show the source at a luminosity level of $\sim 6 \times 10^{34}$ erg s $^{-1}$ in the 3–30 keV interval ($F_{0.3-10\text{keV}} \sim 40 \times 10^{-12}$ erg cm $^{-2}$ s $^{-1}$, unabsorbed). On this occasion, the spectrum was well described by a bare powerlaw continuum with $\Gamma \sim 1.95$, plus a strong (EW ~ 0.75 keV) and broad ($\sigma \sim 0.39$ keV) Gaussian line feature at 6.62 keV, i.e. consistent with a

multi-component or with a relativistically broadened iron line. Significant emission, with no exponential decay, was seen up to 30 keV.

More recently, in October 2000, LS 5039 was observed for 80 ks with *BeppoSAX* by Reig et al. (2003), who found a moderate absorption ($N_H \sim 1 \times 10^{22}$ cm $^{-2}$); however, no iron line was detected, possibly due to the limited signal-to-noise. At the time the source was at a flux level $F_{0.3-10\text{keV}} \sim 4.9 \times 10^{-12}$ erg cm $^{-2}$ s $^{-1}$ (unabsorbed, corresponding to $L_X \sim 5.6 \times 10^{33}$ erg s $^{-1}$ in the 1–10 keV band), almost one order of magnitude lower than in the *Rossi-XTE* observation performed two and a half years before. This negative trend is confirmed also looking at archival 1999 *ASCA* SIS and GIS data (also mentioned by Reig et al., 2003), in which the source has $F_{0.3-10\text{keV}} \sim 13 \times 10^{-12}$ erg cm $^{-2}$ s $^{-1}$. We re-analyzed these data and found they are best fitted by a powerlaw with $\Gamma \sim 1.5$ (see Table 1).

The *BeppoSAX* LECS and MECS continuum was apparently best fitted by a steeper powerlaw ($\Gamma \sim 1.8$). In general, much better constraints on the powerlaw index and, possibly, cutoff energy, are given by the higher-energy *BeppoSAX* camera PDS, which is very well suited to that aim. Unfortunately, the PDS collected too few counts during that observation to provide really useful data. However, the general high-energy spectrum is compatible with a harder powerlaw component ($\Gamma < 1.8$, our analysis). On the base of the orbital solution of McSwain et al. (2001), the covered phase interval seemed favourable to observe an eclipse of the X-ray source by the primary star; the revised ephemeris (McSwain et al. 2004) rather indicates that the *BeppoSAX* observations do not cover periastron, but extend only till slightly before phase 0 (cp. Table 1).

The overall flux history of LS 5039 / RX J1826.2-1450 is summarized in Table 1.

3. Chandra and XMM-Newton observations

In the following we report on recent *Chandra* and *XMM-Newton* observations of LS 5039. Data reduction has been performed with the standard CIAO 3.0 and SAS 6.0 packages, respectively, while for the fitting procedure we used XSPEC 11.2. We tried several spectral models, listed below:

- I. WABS * POWERLAW ;
- IIa. WABS * (POWERLAW + GAUSSIAN) , with $\sigma_{\text{line}} \equiv 0.02$ keV;
- IIb. WABS * (POWERLAW + GAUSSIAN) , with $\sigma_{\text{line}} \equiv 0.39$ keV like in Ribó et al. (1999) ;
- IIIa. WABS * (DISKBB + GAUSSIAN) , with $\sigma_{\text{line}} \equiv 0.02$ keV;
- IIIb. WABS * (DISKBB + GAUSSIAN) , with $\sigma_{\text{line}} \equiv 0.39$ keV like in Ribó et al. (1999) ;
- IV. WABS * (POWERLAW + BBODYRAD) .

The results of the fits are shown in Table 2. Unless stated otherwise, errors are given at the 90 % confidence level. We also tried a model similar to model IV replacing

the blackbody by a disk blackbody for the *XMM-Newton* data (see text below).

3.1. *Chandra*

LS 5039 was observed with *Chandra* ACIS on 2002, September 10, for about 10 ks (06:44:00–10:05:10 UT) in Faint Mode, through the High Energy Transmission Grating (HETG). We analysed the zeroth-order image, with slightly more than 1000 source counts registered, corresponding – when a simple powerlaw continuum is assumed (model I) – to an unabsorbed flux level of $\sim 6.8 \times 10^{-12}$ erg cm $^{-2}$ s $^{-1}$ in the 2 to 10 keV band, equivalent to $\sim 8.1 \times 10^{-12}$ erg cm $^{-2}$ s $^{-1}$ in the 0.3 – 10 keV interval. This is slightly more than in the 2000 *BeppoSAX* pointing, which therefore corresponded to the lowest observed state of this source. However, the spectrum is the hardest in the *Chandra* observation ($\Gamma \sim 1.1$, see Table 1).

We rebinned the ACIS spectrum to a minimum of 25 counts/bin and tried to fit the data by adding an iron line and thermal disk emission (see Table 2). Although the signal-to-noise ratio of the observation is rather poor, we can set some constraints on individual spectral components: in particular, a narrow ($\sigma = 20$ eV) or broad ($\sigma = 390$ eV) Fe line is always compatible (within the 90 % confidence level) with having a null EW, and the F-test shows that its introduction never gives a significantly better fit.

Parameters cannot be really constrained in the powerlaw-plus-blackbody model. The statistics are also too poor to extract any useful information on short-time variability and/or X-ray pulsations.

3.2. *XMM-Newton*

Two pointings of LS 5039 were performed by *XMM-Newton* in 2003: the first one took place on March 8 (07:33:27–10:28:38 UT), the second on March 27 (20:53:47–23:48:59 UT). We analysed EPIC pn (6935 and 6981 counts), MOS1 (3979 and 3437 counts) and MOS2 (3461 and 3521 counts) events. The pointings were performed with Medium filters on; the observing modes were Prime Small Window (time resolution ~ 6 ms) and Prime Partial W2, for the pn and MOS cameras respectively. Too few counts were collected in the RGS cameras to get any useful information. We checked for high background phases, and chose not to set any time filtering given the very modest disturbance (the overall MOS background flux was about 5% of that of the source).

We rebinned the spectrum to a minimum of 20 counts/bin and fitted the data from the three instruments together, with the same models used for the *Chandra* data.

A simple powerlaw provides a good fit to the combined EPIC data for both observations (Figure 1). Again, a (narrow or broad) Fe line has a null EW within the 90% confidence level. There is no evidence of edges or fluorescent lines at lower energies either, which would

have given information on the possible cold surrounding medium (e.g. the stellar wind). On the other hand, *XMM-Newton* throughput and sensitivity at the lowest energies allow better constraints on the hydrogen column density: we get $N_{\text{H}} = 0.70 \pm 0.05 \times 10^{22}$ cm $^{-2}$ in powerlaw models (I and II).

Model III is compatible with a lower N_{H} value. However, this model – pure disk thermal emission – is less plausible both from the physical and the statistical point of view: on one hand, it cannot account for plasma contributions, such as a Comptonization tail; on the other hand, the resulting parameters have no meaning in such low accretion regime (from our fits the resulting innermost radius temperatures are unphysically high). Besides, by adding a disk multi-blackbody component over the powerlaw we obtain negligible normalisations for the thermal emission ($L_{\text{diskbb}}/L_{\text{total}} < 0.09$ and 0.20 , in the two observations respectively). We therefore conclude that there is no evidence of disk emission.

The addition of a simple blackbody on the top of the powerlaw component (model IV) does not improve the fit in a statistically significant manner, either, with respect to the single powerlaw model: the corresponding blackbody radius is consistent with zero at the 90% confidence level. By fixing the blackbody temperature at a more realistic value – e.g. 0.2 keV – the best-fit upper limit on the radius of the blackbody-emitting surface is ~ 1.0 and ~ 1.4 km, in the two observations respectively.

Assuming a simple powerlaw continuum (model I), the unabsorbed 2–10 keV flux is $F_{0.3-10\text{keV}} \sim 10.3$ and 9.7×10^{-12} erg cm $^{-2}$ s $^{-1}$, for the first and second observation respectively. Therefore, LS 5039 did not vary over the 19 day time interval and was still a factor ~ 4 fainter than in the 1998 *Rossi-XTE* observation. Nevertheless, the slow increase of the source X-ray luminosity since the 2000 *BeppoSAX* observation seems confirmed.

The powerlaw index Γ is now ~ 1.5 , as typical of most X-ray binaries in the hard/low state. To make a comparison with other radio-emitting HMXBs, we note that this value is similar to the value of Γ in a radio-outburst phase of LSI +61°303 (Massi 2004) and to that of Cygnus X-1 in some of the low state observations (e.g. Di Salvo et al., 2001).

In order to search for pulsations, we applied the Z_1^2 (Rayleigh) test (see e.g. Zavlin et al. 2000, and references therein) on the events collected by EPIC pn in a narrow circle centred on the source. We found no significant peaks in the Z_1^2 “forest” in the frequency range 0.001–83 Hz: in both observations, upper limits on the pulsed fraction can be set at $f_{\text{P}} \lesssim 10\%$, whereas a rejection at the 3σ level would have corresponded to $f_{\text{P}} < 11.3\%$.

As far as the short time scale variability is concerned, the lightcurves only show slight variation during each pointing (see Figure 2), with no evidence of aperiodic random fluctuations typical of wind accretors. The latter usually display flaring with flux changes of a factor ~ 5 over timescales of a few hundred seconds: we tried with differ-

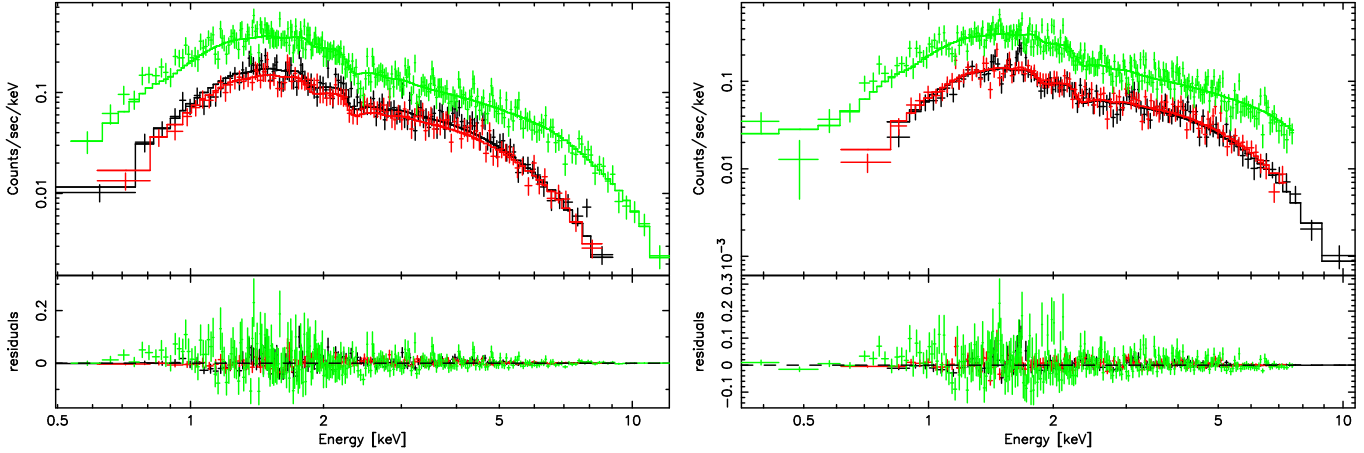


Fig. 1. PN, MOS1 and MOS2 2003 March 8 (left) and March 27 (right) data of LS 5039 / RX J1826.2-1450 are well fitted with an absorbed powerlaw (model I).

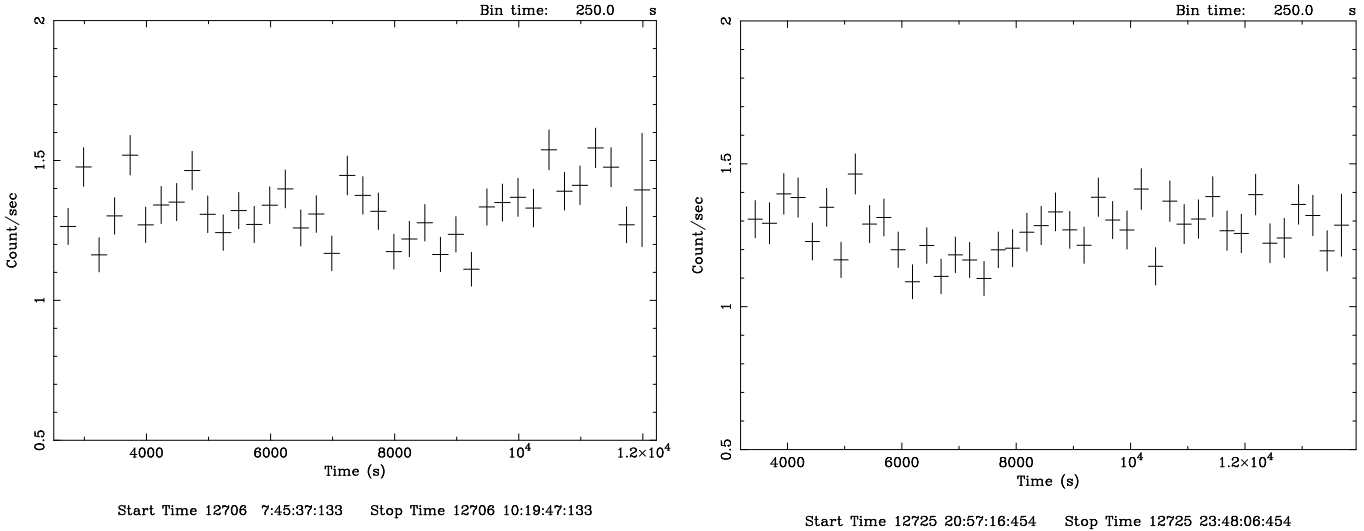


Fig. 2. All-camera, 0.3–7.5 keV lightcurves of the two observations performed with *XMM-Newton*, respectively on 2003 March 8 (left) and on March 27 (right). Notice that in correspondence of a binning time of 250 s, the maximum variation is at the 20% level.

ent binnings (in the range 10–1000 s) and found fluctuations of $\sim 20\%$.

4. Discussion

LS 5039 / RX J1826.2-1450 has been observed with all major X-ray telescopes since its identification in 1997: after its discovery with *ROSAT*, the source was found in a similar state by *Rossi-XTE* in 1998. At that time its luminosity was about a factor 1000 lower than that of classical HMXBs accreting by Roche-lobe overflow, and in the low-end of the distribution of massive binaries fed by wind accretion. This luminosity is comparable to those of Be/X-ray binaries in the low state, but, unlike most of them, LS 5039 displays no detectable X-ray pulsations, and the primary star, identified as a O6.5V(f), does not show evidence of large amount of circumstellar material in the optical.

If the association with the corresponding *EGRET* source is correct, the X-ray luminosity is even smaller than the γ -ray luminosity. A similar situation occurs only in another radio-emitting HMXB, LSI +61°303 (see Massi et al. 2001, Massi 2004, and references therein). LSI +61°303 seems to contain a neutron star, although it shows no pulsations nor high energy cutoff up to $E \sim 25$ keV (see discussion in Greiner & Rau, 2001). Its primary is a Be star with a slowly expanding equatorial envelope from which a transient accretion disk could form at some orbital phases. The strong emission lines from the disk-like equatorial outflow may mask the signature of the compact object, although a weak component moving with the orbital period has probably been detected (Liu et al. 2000; Zamanov & Martí 2000).

4.1. A wind accretor?

The orbital solution (relatively long orbital period) and the lack of ellipsoidal variations in the optical (Martí et al. 2004) exclude the presence of a Roche-lobe overflow. It is thus likely that accretion takes place through stellar wind. This assumption is compatible with the low observed source X-ray luminosity (Mc Swain & Gies 2002).

LS 5039 has been faint in the X-rays since its discovery, but has been emitting steadily in the radio band. Classical accretion theory apparently does not provide a way to form a large and stable accretion disk in a system with the orbital parameters of LS 5039 since the material in the wind carries too little angular momentum. Although small transient discs with different rotation directions may form in such configurations, the discs may be too small to account for the ejection process seen in radio (see e.g. Ruffert 1999). LS 5039 could thus be a rare case in which symmetric, collimated jets form without the help of a well formed accretion disk.

On the other hand, the non-detection of broad optical lines moving with the X-ray source (Clark et al. 2001) is still no proof of the absence of a large disk, for instance due to the strong photospheric continuum of the star; and at present, the general understanding of the processes leading to the formation of bipolar outflows includes the idea that jets are indeed intimately linked to an accretion disk around a potential well. Accretion does not need to be super-Eddington to produce jets. The fact that the observed jet velocity in all sorts of physical situations (from the pre-main-sequence-stars up to the most extreme quasars) scales with the escape velocity suggests that they take their origin close to the compact object (see e.g. Livio 1997). The persistent non-thermal radio emission of LS 5039 is reminiscent of the prototype BH candidate (HMXB) Cygnus X-1, whose radio jet probably also originates in the accretion disk.

A similar, “difficult” case is that of SS 433, also one of the few known radio-emitting HMXB (together with LS 5039, Cyg X-1, Cyg X-3, CI Cam and LSI +61°303; but see Charles & Coe 2003, for a more precise classification and discussion). In this source the X-ray luminosity is $\sim 10^{35}$ erg s⁻¹, not far away from that of LS 5039. However, an accretion disk is clearly detected in the spectra of SS 433, and strong red- and blue-shifted lines are prominent in the optical spectrum. The energy budget at the impact point of the jet with the interstellar medium yields a jet mechanical energy of $\sim 10^{40}$ erg s⁻¹, clearly indicating that SS 433 transforms most of its accretion energy into kinetic energy and that, therefore, only a very small fraction of the accretion power is radiated in the X-rays.

Long term changes in the X-ray flux appear to be correlated with the equivalent width of the H α line (Reig et al., 2003, and McSwain et al., 2004): this favours an explanation of the variation in terms of mean wind density changes. Alternatively, the explanation could lie in the

fact that the X-ray luminosity of a NS or a BH accreting from the high velocity wind of the primary star should vary with orbital phase. In fact, the entire flux range spanned by the source since its discovery (a factor ~ 10 , see Table 1) could be perhaps explained by differences in the orbital phases of the various observations (Reig et al., 2003); and one could note that, assuming the revised ephemeris of McSwain et al. (2004), the X-ray brightest *Rossi-XTE* observations took place at a phase closest to periastron passage (see Table 1). However, apart from a number of complications observed in other sources, which may question this interpretation,¹ the already mentioned *BeppoSAX* results (Reig et al. 2003) when combined with the ephemeris of McSwain et al. (2004) are clearly inconsistent with the hypothesis that orbital modulation play a major role, since the lightcurve only shows a steady flux decrease whereas the flux should peak close to periastron.

The original period of McSwain et al. (2001) used to plan the two *XMM-Newton* observations predicts orbital phases of 0.95 and 0.70 for the 2003 March 8 and 27 observations respectively, in which case a large flux variation would have been expected. However, according to the revised ephemeris of McSwain et al. (2004), the phases of the first and second *XMM-Newton* observations are now 0.79 and 0.21, i.e. at symmetric times before and after the periastron passage, and should therefore show similar fluxes, as actually observed. However, since other 4-d alias orbital periods may not be ruled out yet, we believe that it is still difficult, at present, to completely distinguish between orbital and long-term wind variability.

The total absorption of LS 5039 has been better constrained by *XMM-Newton*, thanks to the satellite’s sensitivity at low energies. We obtain values around $N_{\text{H}} \sim 7 \times 10^{21}$ cm⁻². This is comparable to the values derived from optical reddening observations (see Introduction), and approaches the value estimated for the total galactic interstellar absorption in the same direction ($N_{\text{H}} \sim 8.7 \times 10^{21}$ cm⁻²; Dickey & Lockman 1990). Therefore, contrary to the comparable case of 4U 1700-37 (Hammerschlag-Hensberge et al. 1990), no large variable local absorption is seen in LS 5039, at least at the time of the *XMM-Newton* observations.

4.2. The young pulsar scenario

The nature of the compact object in LS 5039 still remains an unsolved issue. Although the hypothesis of a central black hole cannot be ruled out, the orbital solution rather favours a neutron star assumption. This would not contradict the non-detection of pulsations, as shown e.g. by the cases of 4U 2206+54 (Torrejón et al. 2004) and 4U 1700-

¹ For instance, the fact that the orbital X-ray lightcurve of the wind accreting source GX 301-2 peaks about 0.07 in phase before periastron as a result of wind rotation and stream flows within the system (Leahy 2002).

37, which are HMXBs too. However, the latter two objects show some differences with respect to LS 5039, including the fact that they are not radio sources. The only neutron star candidate, radio-emitting HMXB which shows no pulsations, together with LS 5039, is precisely LSI+61°303.

Proper motion, measured in the radio and optical domain, together with optical radial velocities indicate that LS 5039 is escaping its local standard of rest with a high kick velocity of $\sim 150 \text{ km s}^{-1}$ (Ribó et al. 2002). These authors conclude that its present height above the galactic plane is consistent with a maximum age of about $1.1 \times 10^6 \text{ yr}$. If the accreting companion were a neutron star it would therefore be a young or, at most, a middle-aged pulsar.

Let us briefly discuss the hypothesis of a very young neutron star. It may be still rotating too fast to accrete, and be in the propeller regime; this mechanism is still not understood in detail and it is difficult to say whether the inferred X-ray properties would be consistent with the observations. It is believed that such a mechanism can give rise to fast ejection, but, considering the strong influence of the high-mass companion wind, it is unclear whether symmetric, well collimated jets could be generated.

Young neutron stars have spin-down luminosities which can be comparable with the total estimated radio plus X-ray plus γ -ray luminosity radiated by the companion of LS 5039 (a few $10^{35} \text{ erg s}^{-1}$), and their ages are still consistent with the absence of existing nearby SNR (see e.g. Becker et al. 2002). The possibility thus remains that part of the observed luminosity is actually extracted from the relativistic wind of a pulsar which carries away most of the rotational energy, instead of being due to accretion onto the compact object or on its magnetosphere if propeller effects dominate. In the case of the binary pulsar PSR 1259–63 (spin down age $3 \times 10^5 \text{ yr}$ and spin down luminosity of $8 \times 10^{35} \text{ erg s}^{-1}$) orbiting a Be star, Tavani and Arons (1997) argue that shock powered emission in a pulsar wind termination shock at a large distance can account for the observed X-ray luminosity of a few $10^{34} \text{ erg s}^{-1}$ through various mechanisms (see also Murata et al., 2003, and references therein).

In the case of the Be system LSI+61°303, which displays radio, X-ray and possibly also γ -ray luminosities similar to LS 5039, Harrison et al. (2000) propose that X-ray and γ -ray emission arises from inverse Compton scattering of stellar photons on electrons accelerated in the shock between the stellar wind and the pulsar wind. The origin and composition of the latter (hadrons or only leptons?) should be investigated, as well as the conditions under which the relativistic pulsar wind would be actually able to create a cavity within the stellar wind.² Such a cavity should be symmetric and large enough to account for the shape and size of the ejections which are

observed in the radio band: this is an open issue, still to be addressed by proper modelling. The recent discovery of radio jets in LSI+61°303, with a geometry and size ($\sim 0.01 \text{ pc}$) quite similar to those seen in LS 5039, has been considered to argue against the wind shock mechanism and for an accretion-ejection process (Massi et al. 2004). We note, however, that young neutron stars such as the Vela pulsar can produce well formed jets visible in X-rays (Pavlov et al. 2003): such jets are thought to be associated with collimated outflows of relativistic particles along the pulsar’s spin axis. In the case of the Vela pulsar, the jet scale is of the order of one parsec, i.e. two orders of magnitude greater than in LSI+61°303 and LS 5039, while the pulsar’s age could be as much as two orders of magnitude less than in the latter sources. At a lower rotational luminosity scale, the distorted shapes of the optical bow shock nebulae of PSR B0740-28 and PSR J2124-3358 rather point towards anisotropy in the pulsar wind, in addition to structures in the ambient ISM (see e.g. Gaensler 2004, and references therein).

The possible lack or weakness of any orbit-related flux variation could also hold as an argument against the accreting neutron star scenario. We are thus perhaps witnessing in LS 5039 the effects of the interaction between the relativistic collimated wind of a young pulsar with the O star wind. It is beyond the scope of this paper to discuss the shock structures and emission mechanism which could account for the radio to γ -ray energy distribution, but we wish, however, to question in this particular case the paradigm which systematically associates bipolar outflows with accretion discs.

4.3. What about the iron line?

The detection by *Rossi-XTE* of a strong, broad fluorescent iron line (Ribó et al. 1999) cannot be confirmed with the better resolution X-ray data provided by *Chandra* and *XMM-Newton*, and this is apparently not just due to poor statistics in such faint states. The broad line component ($\sigma_{\text{line}} = 390 \text{ eV}$) claimed by Ribó et al. (1999) has null equivalent width even within the 99% confidence level in *XMM-Newton* data, with an upper limit of 0.14 keV compared to the 0.75 keV observed by Ribó et al. (1999). F-tests lead to exclude all broad line as well as narrow line models (IIa,b and IIIa,b) with high confidence. Let us shortly comment on this.

The detection and the study of fluorescent iron emission in accreting galactic BH candidates can be a powerful tool to test assumptions on the extreme gravitational field as well as on the accretion/ejection flows which are present in the innermost parts of such systems, at just a few gravitational radii ($r_g = GM/c^2$) from the BH horizon or compact object surface.³ This was first demonstrated

² This may be a greater problem in the case of Be stars, whose equatorial outflows are assumed to be denser than in the case of O-type stars. The effect of the orbital eccentricity would make a difference, too.

³ See e.g. Reynolds & Nowak (2002) for a review on fluorescent iron lines as a probe of astrophysical BH systems, and Martocchia, Karas & Matt (2000) on details about the Fe line diagnostics in the “cold” disk assumption.

by the case of some Active Galactic Nuclei (e.g. Tanaka et al. 1995), but soon observational campaigns of galactic BH candidates, performed with all recent X-ray satellites, showed that broad, intense Fe lines are not rare in stellar-mass sources. However, such phenomenon generally occurs in “intermediate / very high” spectral states, while after 1999 LS 5039 / RX J1826.2-1450 has been observed always in a “low/hard” state.

Broad lines, best-fitted with a relativistic disk model, have been observed among others in Cygnus X-1, XTE J1650-500, V4641 Sgr, XTE J2012+381. In the cases of XTE J1650-500 and GX 339-4, *XMM-Newton* detected very broad, skewed lines, best-fitted with a canonical Kerr innermost stable orbit, and a very steep emissivity profile (Miller et al. 2002 and 2004). GRS 1915+105, too, showed a broad, distorted iron line in a few *BeppoSAX* observations (Martocchia et al., 2002 and 2004). In other sources, the lines and their profiles are rather interpreted as products of ejected material: besides XTE J1550-564 and 4U 1630-47, this is the case of SS 433, where two (red- and blue-shifted) iron line components are visible, which follow the same velocity variations of several other emission lines, observed with ASCA SIS and Chandra HETGS (see Kotani et al. 1994 and Marshall et al. 2002, respectively). A broad, relatively intense fluorescent iron line has been observed in CICam as well, with various instruments including *XMM* (e.g. Ueda et al. 1998, Boirin et al. 2002).

The line observed with the PCA onboard *Rossi-XTE*, if confirmed by an X-ray observation of the source in a brighter state, could have a disk or a jet origin. In the first case, the line may carry the general-relativistic imprints of the strong gravitational potential well in the vicinity of compact objects; and the blue-shift – 6.6 instead of the 6.4 keV iron $K\alpha$ rest energy – would imply a substantial disk ionisation. In the disk assumption, the fact that the line is not seen in the faintest states could be a consequence of the disk disappearance in the “jet” (low/hard) state. On the other hand, in galactic stellar-mass sources the ionisation of the accreting flow is thought to be much more relevant than in Active Galactic Nuclei because of the much larger disk temperature in stellar size objects; this sometimes results in fluorescent emission being less effective. Moreover, the non-negligible X-ray variability of such sources, which reflects rapid changes in the physics and geometry of the accretion/ejection phases, also causes the iron emission to be non-steady, and even non-detectable in many situations.

If emitted from a jet, instead, the line would be shifted in energy mainly as a consequence of the Doppler effect, due to the bulk velocity of the jet material, and the broadening may be interpreted as a signature of the jet opening angle. The jet matter, on its account, must be “cold” to emit the line efficiently. Since in the case of LS 5039 the radio-observed ejections are symmetric (Paredes et al. 2000, 2002), the issue would be to self-consistently explain why the line is observed in only one of the two jets. The

fact that this is the jet approaching the observer leads us to invoke Doppler boosting.

In absence of pulsations, lacking a precise determination of the compact object’s mass, and since we have no indications on the presence or absence of a high-energy cutoff, the iron line diagnostics would be crucial to investigate the nature of the compact object. A dedicated *XMM-Newton* observation to catch the source in a bright, Fe line-emitting state was proposed also for AO3. The idea is to trigger the observation by optical monitoring, using the fact that an anticorrelation between the measured (negative) EW($H\alpha$) and the observed X-ray flux – as claimed by Reig et al. (2003) – is likely due to the connection between the primary mass-loss rate (which governs the optical emission) and the mass accretion rate onto the compact object (which governs the X-rays). However, LS 5039 / RX J1826.2-1450 has failed to enter such a “bright” state, requested as a triggering condition, up to now.

5. Conclusions

Recent *XMM-Newton* and *Chandra* observations of LS 5039 / RX J1826.2-1450 caught the source in a faint state. The X-ray spectrum can be fitted by an absorbed powerlaw, without the need for any disk component. Simple blackbody emission, which could be generated at a neutron star’s surface, is ruled out, too. The powerlaw shape is hard ($\Gamma = 1.1 \div 1.5$), similar to that of most X-ray binaries in the low/hard state.

In contrast to previous *RXTE* observations, we do not find any evidence of iron line emission. Even if the iron line in LS 5039 / RX J1826.2-1450 is a transient feature, data from satellites with better sensitivity and resolution, observing the source in a brighter state, would be necessary to confirm or reject the *Rossi-XTE* claim.

XMM-Newton data allow a better constraint on the hydrogen column density ($N_{\text{H}} \sim 7 \times 10^{21} \text{ cm}^{-2}$), excluding the presence of large amounts of local absorption at the time of these observations.

The absence of pulsations down to low pulse fractions is confirmed. We also fail to detect the flaring activity often seen in wind accreting systems: the X-ray flux of the source varies by just $\sim 20\%$ on timescales of a few hundred seconds within each *XMM-Newton* observation.

The overall flux history of the source is summarized in Table 1. While a general correlation is possible, and can be seen (although not so strict) between spectral “hardness” and X-ray flux, the latter shows no clear dependence on the orbital phase, assuming the ephemeris by McSwain et al. (2004). Although part of the long term flux variations still could be due to orbital effects in a wind accretion scenario, many other arguments rather favour an interpretation not based on accretion. They include: the likely physical impossibility of forming a large disk with the given orbital parameters; the non-detection of disk spectral features; the apparent lack of intrinsic absorption, and the non-detection of edges or fluorescent lines in

the soft X-rays, which would have given information on the stellar wind.

We therefore discussed the hypothesis that LS 5039/RX J1826.2-1450 may be a young pulsar, and that X-ray emission may arise from the interaction between its relativistic collimated wind and the wind of the primary star. This would break the paradigm which systematically associates bipolar outflows with the presence of an accretion disc. X-ray observations spanning a complete orbital period, possibly accompanied by optical monitoring of the H α feature, are strongly needed to finally discriminate between the various models for the accretion/ejection mechanism as well as for the nature of the compact object in LS 5039/RX J1826.2-1450.

Acknowledgements. The authors are grateful to the anonymous referee, to Marc Ribó and to Slava Zavlin for their useful comments and suggestions. AM also wishes to thank Giorgio Matt for the help, and CNES for financial support. IN is a researcher of the programme *Ramón y Cajal*, funded by the Spanish Ministerio de Ciencia y Tecnología and the University of Alicante. This research is partially supported by the Spanish Ministerio de Ciencia y Tecnología under grant ESP2002-04124-C03-03.

References

- Becker, W. & Aschenbach, B. 2002, in: Proc. 270th WE-Heraeus Seminar on Neutron Stars, Pulsars, and Supernova Remnants. MPE Report 278. Edited by W. Becker, H. Lesch, and J. Trümper. Garching bei München: Max-Planck-Institut für extraterrestrische Physik, p.64
- Boirin, L., Parmar, A.N., Oosterbroek, T., Lumb, D., Orlandini, M., Schartel, N. 2002, A&A 394, 205
- Bosch-Ramon, V. & Paredes, J.M. 2004, A&A 417, 1075
- Charles, P.A. & Coe, M.J. 2003, in: *Compact Stellar X-ray Sources*, eds. W.H.G. Lewin & M. van der Klis, in press – astro-ph/0308020
- Clark, J.S., Reig, P., Goodwin, S.P. et al. 2001, A&A 376, 476
- Dickey, J.M. & Lockman, F.J. 1990, ARAA 28, 215
- Di Salvo, T., Done, C., Zycki, P.T., Burderi, L., Robba, N.R. 2001, ApJ 547, 1024
- Gaensler, B.M. 2004, IAU Symp Vol. 218, F.Camilo & B.M. Gaensler Eds – astro-ph/0405290
- Greiner J. & Rau A. 2001, A&A 375, 145
- Hammerschlag-Hensberge, G., Howarth, I.D., Kallman, T.R. 1990, ApJ 352, 698
- Harrison, F.A., Ray, P.S., Leahy, D.A., Waltman, E.B., Pooley G.G. 2000, ApJ 528, 454
- Howarth, I.D. & Prinja, R.K. 1989, ApJ Suppl. 69, 527
- Kotani, T. et al. 1994, PASJ 46, L147
- Leahy, D.A. 2002, A&A 391, 219
- Liu, Q.Z. et al. 2000, A&A 359, 646
- Livio, M. 1997, ASP Conf. Series 121, 845
- Marshall, H.L., Canizares, C.R., Schulz, N.S. 2002, ApJ 564, 941
- Martí, J., Paredes, J.M., Ribó, M. 1998, A&A 338, L71
- Martí, J., Luque-Escamilla, P., Garrido, J.L., Paredes, J.M., Zamanov, R. 2004, A&A 418, 271
- Martocchia, A., Karas, V., Matt, G. 2000, MNRAS 312, 817
- Martocchia, A., Matt, G., Karas, V., Belloni, T., Feroci, M. 2002, A&A 387, 215
- Martocchia, A., Matt, G., Karas, V., Belloni, T., Feroci, M. 2004, in: Proc. II BeppoSAX Symposium, *The restless high-energy universe*, Amsterdam (The Netherlands), 5-8/5/2003. Eds. E.P.J. Van den Heuvel, J.J.M. In't Zand and R.A.M.J. Wijers, published by Elsevier, Nucl. Physics B Suppl. Ser, in press
- Massi, M., Ribó, M., Paredes, J.M., Peracaula, M., Estalella, R. 2001, A&A 376, 217
- Massi, M. 2004, A&A 422, 267
- Massi, M., Ribó, M., Paredes, J.M., Garrington, S.T., Peracaula, M., Martí, J. 2004, A&A 414, L1
- McSwain, M.V. & Gies, D.R. 2002, ApJ 568, L27
- McSwain, M.V., Gies, D.R., Riddle, R.L., Wang, Z., Wingert D.W. 2001, ApJ 558, L43
- McSwain, M.V., Gies, D.R., Huang, W., Wiita, P.J., Wingert, D.W., Kaper, L. 2004, ApJ 600, 927
- Miller, J.M. et al. 2002, ApJ 570, L69
- Motch, C., Haberl, F., Dennerl, K., Pakull, M., Janot-Pacheco, E. 1997, A&A 323, 853
- Murata, K., Tamaki, H., Maki, H., Shibazaki, N. 2003, PASJ 55, 473
- Paredes, J.M., Martí, J., Ribó, M., Massi, M. 2000, Science 288, 2340
- Paredes, J.M., Ribó, M., Ros, E., Martí, J., Massi, M. 2002, A&A 393, L99
- Pavlov, G.G., Teter, M.A., Kargaltsev, O., Sanwal, D. 2003, ApJ 591, 1157
- Predehl, P. & Schmitt, J.H.M.M. 1995, A&A 293, 889
- Reig, P., Ribó, M., Paredes, J.M., Martí, J. 2003, A&A 405, 285
- Reynolds, C.S. & Nowak, M.A. 2003, Phys. Reports 377, 389
- Ribó, M., Reig, P., Martí, J., Paredes, J.M. 1999, A&A 347, 518
- Ribó, M., Paredes, J.M., Romero, G.E. et al. 2002, A&A 384, 954
- Ruffert, M. 1999, A&A 346, 861
- Tanaka, Y. et al. 1995, Nature 375, 659
- Tavani, M. & Arons, J. 1997, ApJ 477, 439
- Torrejón, J.M., Kreykenbohm, I., Orr, A., Titarchuk, L., Negueruela, I. 2004, A&A 423, 301
- Ueda, Y., Ishida, M., Inoue, H., Dotani, T., Greiner, J., Lewin, W.H.G. 1998, ApJ 508, L167
- Zamanov, R. & Martí, J. 2000, A&A 358, L55
- Zavlin, V.E., Pavlov, G.G., Sanwal, D., Trümper, J. 2000, ApJ 540, L25
- in't Zand, J.J.M. et al. 2000, A&A 357, 526

	<i>Chandra</i> , 10/09/02	<i>XMM-Newton</i> , 08/03/03	<i>XMM-Newton</i> , 27/03/03
actual duration [s] count rate [s ⁻¹]	10608 0.094 ± 0.003	~ 10650 (MOS), 10510 (pn) 0.919 ± 0.012 (pn)	~ 10665 (MOS), 10510 (pn) 0.878 ± 0.012 (pn)
model I	61.7/44 = 1.40	465.7/478 = 0.97	510.0/460 = 1.11
N_{H} [10 ²² cm ⁻²] Γ	0.56 ^{+0.35} _{-0.19} 1.15 ^{+0.23} _{-0.21}	0.72 ^{+0.03} _{-0.05} 1.56 ^{+0.02} _{-0.05}	0.69 ^{+0.05} _{-0.03} 1.49 ^{+0.05} _{-0.04}
model IIa (narrow line)	61.7/43 = 1.43	465.4/477 = 0.98	510.8/459 = 1.11
N_{H} [10 ²² cm ⁻²] Γ	0.58 ^{+0.35} _{-0.29} 1.17 ^{+0.23} _{-0.22}	0.69 ^{+0.05} _{-0.02} 1.53 ^{+0.04} _{-0.04}	0.70 ^{+0.05} _{-0.03} 1.50 ^{+0.03} _{-0.05}
E_0 (Fe K α) [keV] EW(Fe K α) [eV] σ (Fe K α) [eV]	6.4 (fixed) 5 ⁺²⁸⁸ ₋₅ 20 (fixed)	6.4 (fixed) 0(< 1) 20 (fixed)	6.4 (fixed) 0(< 87) 20 (fixed)
model IIb (broad line)	61.5/43 = 1.43	465.5/477 = 0.98	510.8/459 = 1.11
N_{H} [10 ²² cm ⁻²] Γ	0.60 ^{+0.40} _{-0.32} 1.20 ^{+0.27} _{-0.26}	0.69 ^{+0.05} _{-0.02} 1.53 ^{+0.04} _{-0.04}	0.70 ^{+0.05} _{-0.04} 1.50 ^{+0.04} _{-0.04}
E_0 (Fe K α) [keV] EW(Fe K α) [eV] σ (Fe K α) [eV]	6.4 (fixed) 165 ⁺⁵⁶⁴ ₋₁₆₅ 390 (fixed)	6.4 (fixed) 0(< 137) 390 (fixed)	6.4 (fixed) 0(< 187) 390 (fixed)
model IIIa (narrow line)	56.9/42 = 1.35	566.0/477 = 1.19	539.4/459 = 1.18
N_{H} [10 ²² cm ⁻²] T (blackbody) [keV]	0.28 ^{+0.16} _{-0.14} 3.85 ^{+0.77} _{-0.67}	0.44 ^{+0.03} _{-0.02} 2.34 ^{+0.08} _{-0.09}	0.45 ^{+0.04} _{-0.02} 2.29 ^{+0.09} _{-0.09}
E_0 (Fe K α) [keV] EW(Fe K α) σ (Fe K α) [eV]	7.04 ^{+0.20} _{-1.67} 331 ^{+E13} ₋₃₃₁ 20 (fixed)	6.4 (fixed) 0(< 82) 20 (fixed)	6.4 (fixed) 0(< 97) 20 (fixed)
model IIIb (broad line)	58.4/42 = 1.39	566.0/477 = 1.19	537.0/459 = 1.17
N_{H} [10 ²² cm ⁻²] T (blackbody) [keV]	0.32 ^{+0.16} _{-0.14} 3.39 ^{+0.89} _{-0.55}	0.44 ^{+0.03} _{-0.02} 2.34 ^{+0.08} _{-0.09}	0.48 ^{+0.02} _{-0.08} 2.18 ^{+0.09} _{-0.10}
E_0 (Fe K α) [keV] EW(Fe K α) σ (Fe K α) [eV]	7.09 ^{+1.01} _{-0.53} 699 ^{+E13} ₋₆₉₉ 390 (fixed)	6.4 (fixed) 0(< 149) 390 (fixed)	6.4 (fixed) 0(< 472) 390 (fixed)
model IV	–	460.2/476 = 0.97	503.5/458 = 1.10
N_{H} [10 ²² cm ⁻²] Γ T (blackbody) [keV] r (blackbody) [km]	– – – –	0.67 ^{+0.04} _{-0.08} 1.53 ^{+0.04} _{-0.04} 0.95 ^{+0.13} _{-0.19} 0(< 0.07)	0.66 ^{+0.10} _{-0.05} 1.52 ^{+0.15} _{-0.06} 1.14 ^{+0.09} _{-0.16} 0(< 0.05)

Table 2. Best-fit parameters for the spectral models listed at the end of Section 2. χ^2/dof values are given in correspondence of each model's name and for each observation.